7

Sliding Mode Control of Robot Manipulators via Intelligent Approaches

Seyed Ehsan Shafiei
Shahrood University of Technology
Iran

1. Introduction

1.1 Robot manipulators

Robot manipulators are well-known as nonlinear systems including strong coupling between their dynamics (Craig, 1996). These characteristics, in company with: 1) *structured uncertainties* caused by model imprecision of link parameters, payload variation, etc., and 2) *unstructured uncertainties* produced by un-modeled dynamics –such as nonlinear friction and external disturbances– make the motion control of rigid-link manipulators a complicated problem (Spong & Vidiasagar, 1989). Practice trajectory control is required in many of the sophisticated applications of manipulators (e.g. machining, welding, complex assembly). On the other hand, robot manipulators have to face various uncertainties in their dynamics and they are required to handle various tools and, hence, the dynamic parameters of the robots vary during operation. Thus, it is difficult to initiate an appropriate mathematical model for employing model-based control strategies.

In general, the intelligent control approaches can attenuate the effects of structured parametric uncertainty and unstructured disturbance by using their powerful learning ability without a detailed knowledge of the controlled plant in the design processes. On the other hand, many intelligent control algorithms could have been found for the robot control system without including the actuator dynamics, while, actuator dynamics carry out a significant role in the complete robot dynamics and ignoring them may cause detrimental effects, especially in the case of high-velocity moment, highly varying loads, friction, and actuator saturations (Chang et al., 2008), (Chang & Yen, 2009). Since the electrical actuators are highly controllable in comparison with the other one, they are more convenient for driving manipulators. Also, in practical applications, the voltages or currents of the electrical actuators are accessible for applying control commands and consequently, torque-based control design confronts implementation problems when one intends to apply the torque control commands directly to actuators. Additionally, one constraint in the robot controller designs is saturation nonlinearity of actuators which is less considered in control design of robot manipulators.

1.2 Sliding mode control

Sliding mode control (SMC) is a variable-structure, robust control strategy which is capable in controlling different class of uncertain systems including nonlinear systems, MIMO systems, and even discrete time systems (Utkin, 1978), (Zhang et al., 2008). Such

uncertainties may be structured, unstructured, or may result from nondeterministic features of the plant. A sliding mode controller is essentially high gain switching controller. The idea is to keep the trajectory of the system on a particular surface in the phase space. In a two dimensional system this would reduce to following a line in the phase plane. The SMC law is formulated using a Lyapunov approach that guarantees robustness despite the presence of bounded modeling uncertainties (Slotin & Li, 1991).
However, sliding mode control has a good deal of advantages such as insensitivity to parameter variations, disturbance rejection and fast dynamic responses (Zhang et al., 2008). Despite these merits, SMC suffers from some disadvantages. Actually, the sliding mode control law consists of two main parts. The first part is the *equivalent control law* which involves inverse dynamics of model nonlinearities that demonstrates the dependency of SMC on the dynamical model of the plant. The second part is the *robustifying term* which has discontinuous nature and may employ unnecessary high control gain to overcome uncertainties and disturbances. However, this discontinuity may lead to chattering phenomenon that can excite un-modeled high-frequency plant dynamics and harm the overall control system. Also, using high control gain may cause saturating the actuators. Accordingly, several methods have been developed for improving the SMC performance which the most significant of them is intelligent control approach (Kaynak et al., 2001) mainly includes fuzzy logic control and neural network control.

1.3 Fuzzy control

Fuzzy control is based on fuzzy logic and is a nonlinear control strategy which uses heuristic information. In the fuzzy control design methodology, human thinking and expert knowledge are incorporated into a fuzzy system that emulates the decision-making process of the human. Basically, a fuzzy system in general or fuzzy control in especial comprises five main parts: 1) fuzzyfication of inputs, 2) fuzzy control rules, 3) fuzzy implication, 4) fuzzy reasoning and 5) defuzzification (Lee, 1990), (Wang, 1997).
Fuzzy control represents efficient performance in absence of uncertainties and disturbance and where the plant dynamics were well-described with mathematical equations. Moreover, stability of the fuzzy control systems is hard to analyze and needs strong mathematical procedures. Therefore, it seems reasonable to enhance fuzzy control efficiency by using of incorporating well-organized nonlinear control methods (e.g. sliding mode control).

1.4 Neural network control

Prominent features of neural networks (NN) have drawn much attention in control research areas especially in robot control systems (Lewis, 1998). Some of this features that are closely related to control design strategies are:

- *Universal approximation*: neural networks can approximate smooth nonlinear functions with any degree of accuracy. This feature may be utilized in nonlinear control systems.
- *Learning and adaptation*: neural networks can be trained off-line with adequate amount of data or they can be adapted on-line with appropriate adaptation laws. This property is applied to identification concerns.
- *MIMO characteristic*: neural networks can accept many inputs and can produce required number of outputs. So they are appropriate for MIMO control systems.

There are many other distinguished features as parallel processing, hardware implementation and data fusion etc. that we neglect them here. Also, fuzzy logic may be employed for constructing special networks like fuzzy-neural-networks. Alternatively, neural networks may be exerted to fuzzy control design like neuro-fuzzy control systems.

In the reminder of this chapter three methods are proposed for controller designs. In the first case, sliding mode control plays the main role and fuzzy logic is employed for tuning the controller gains. In the second case, fuzzy control and sliding mode control have the parallel mission in control strategy. Finally, the third case proposes the sliding mode control method by using adaptive neural network approach.

2. Sliding mode control using fuzzy approach

2.1 Sliding_mode_PID controller design by using of fuzzy tuning

This section addresses a chattering free sliding mode control (SMC) for a robot manipulator including PID part with a fuzzy tunable gain. The main idea is that the robustness property of SMC and good response characteristics of PID are combined with fuzzy tuning gain approach to achieve more acceptable performance. For this purpose, in the first stage, a PID sliding surface is considered such that the robot dynamical equations can be rewritten in terms of sliding surface and its derivative and the related control law of the SMC design will contain a PID part. The stability guarantee of this sliding mode PID-controller is proved by a lemma using Lyapunov direct method. Then, in the second stage, in order to decrease the reaching time to the sliding surface and deleting the oscillations of the response, a fuzzy tuning system is used for adjusting both controller gains including sliding controller gain parameter and PID coefficients (Ataei & Shafiei, 2008).

2.1.1 Mathematical model of the system

The dynamical equation of an n-link robot manipulator in the standard form is as follows (Spong & Vidiasagar, 1989):

$$M(q)\ddot{q} + C(q,\dot{q})\dot{q} + G(q) + \tau_d = \tau \tag{1}$$

where $M(q) \in R^{n\times n}$ is the completed inertia matrix, the vectors $q,\dot{q},\ddot{q} \in R^n$ are the position, velocity and angular acceleration of the robot joints, respectively. Moreover, the matrix $C(q,\dot{q}) \in R^{n\times n}$ is the matrix of Coriolis and centrifugal forces and $G(q) \in R^n$ is the gravity vector. Also, $\tau_d \in R^n$ denotes the vector of disturbance and un-modeled dynamics, and finally, τ is the torque vector. In the following, two conventional properties of the robot manipulators are considered.

Property 2.1. The inertia matrix $M(q)$ is symmetric and positive definite, $M^T = M$.

Property 2.2. The matrix of $(\dot{M} - 2C)$ is skew-symmetric, i.e. for any vector of X, we have $X^T(\dot{M} - 2C)X = 0$.

2.1.2 Sliding mode control with PID

The objective of the tracking control is to design such a control law, for obtaining the suitable input torque τ, that the position vector q could track the desired trajectory q_d. In this regard, the tracking error vector is defined as follows:

$$e = q_d - q \tag{2}$$

In order to apply the SMC, the sliding surface is considered as relation (3) which contains the integral part in addition to the derivative term:

$$s = \dot{e} + \lambda_1 e + \lambda_2 \int_0^t e dt \tag{3}$$

where λ_i is diagonal positive definite matrix. Therefore, $s = 0$ is a stable sliding surface and $e \to 0$ as $t \to \infty$. The robot dynamical equations can be rewritten based on the sliding surface (in term of filtered error) as:

$$M\dot{s} = -Cs + f + \tau_d - \tau \tag{4}$$

Where

$$f = M(\ddot{q}_d + \lambda_1 \dot{e} + \lambda_2 e) + C(\dot{q}_d + \lambda_1 e + \lambda_2 \int_0^t e dt) + G \tag{5}$$

Now, the control input can be considered as:

$$\tau = \hat{f} + K_v s + K \operatorname{sgn}(s) \tag{6}$$

where

$$\hat{f} = \hat{M}(\ddot{q}_d + \lambda_1 \dot{e} + \lambda_2 e) + \hat{C}(\dot{q}_d + \lambda_1 e + \lambda_2 \int_0^t e dt) + \hat{G} \tag{7}$$

is an estimation of f and $K_v s = K_v \dot{e} + K_v \lambda e + K_v \lambda \int_0^t e dt$ is the outer PID tracking loop, and K_v, K are diagonal positive definite matrices and are defined such that the stability conditions are guaranteed. The sgn(s) is also the sign function.

We have also:

$$\left|\tilde{f}\right| = \left|\tilde{M}(\ddot{q}_d + \lambda_1 \dot{e} + \lambda_2 e) + \tilde{C}(\dot{q}_d + \lambda_1 e + \lambda_2 \int_0^t e dt) + \tilde{G}\right| \le F \tag{8}$$

where $\tilde{f} = f - \hat{f}$, $\tilde{M} = M - \hat{M}$, $\tilde{C} = C - \hat{C}$,and $\tilde{G} = G - \hat{G}$. Vector F can also be selected as the following relation:

$$F = \left|\tilde{M}(\ddot{q}_d + \lambda_1 \dot{e} + \lambda_2 e)\right| + \left|\tilde{C}(\dot{q}_d + \lambda_1 e + \lambda_2 \int_0^t e dt\right| + \left|\tilde{G}\right| \tag{9}$$

In order to govern the system states $(e, \dot{e})$ to reach the sliding surface $s = 0$ in a limited time and to remain there, the control law should be designed such that the following sliding condition is satisfied (Slotin & Li, 1991):

$$\frac{1}{2}\frac{d}{dt}\left[s^T M s\right] < -\eta (s^T s)^{1/2} \ , \quad \eta > 0 \tag{10}$$

This aim is fulfilled in the following lemma.

Lemma 2.1. In the SMC design of a system with dynamical equation (1) and sliding surface (3), if the control input τ is selected as (6), by considering F as (9) and $K = diag(K_{11}, K_{22}, \ldots, K_{nn})$ with the following components:

$$K_{ii} = \left[F + \left|K_v s\right| + T_D + \eta\right]_i \quad , \quad i = 1,2,\ldots,n \tag{11}$$

Then, the sliding condition (10) is satisfied by equation (4).
Proof: Consider the following Lyapunov function candidate:

$$V = \frac{1}{2} s^T M s \tag{12}$$

Since M is positive definite, for $s \neq 0$ we have $V > 0$ and by taking derivative from relation (12) and regarding the symmetric property of M, it can be written:

$$\dot{V} = \frac{1}{2} s^T \dot{M} s + s^T M \dot{s} \tag{13}$$

By substituting (4) into (13) and considering that $s^T(\dot{M} - 2C)s = 0$, we have:

$$\dot{V} = \frac{1}{2} s^T \dot{M} s - s^T C s + s^T(f + \tau_d - \tau) = s^T(f + \tau_d - \tau) \tag{14}$$

By replacing the relation (6) into (14), $\dot{V}$ can be rewritten as:

$$\dot{V} = s^T(f + \tau_d - \hat{f} - K_v s - K\mathrm{sgn}(s)) = s^T(\tilde{f} + \tau_d - K_v s) - \sum_{i=1}^{n} K_{ii}\left|s_i\right| \tag{15}$$

Since the following inequality (16) is valid and by regarding the relation (11), we have:

$$F + \left|K_v s\right| + T_D \geq \left|\tilde{f} + \tau_d - K_v s\right| \tag{16}$$

$$K_{ii} \geq \left|[\tilde{f} + \tau_d - K_v s]_i\right| + \eta_i \tag{17}$$

Finally, it can be concluded that:

$$\dot{V} \leq -\sum_{i=1}^{n} \eta_i \left|s_i\right| \tag{18}$$

This indicates that V is a Lyapunov function and the sliding condition (10) has been satisfied.
The use of sign function in the control law leads to high oscillations in control torque which is undesired phenomenon and is called chattering. To overcome this drawback, there are some solutions that one of them is using the following saturation function instead of sign function in the discontinuous part of the control law:

$$sat\left(\frac{s}{\varphi}\right) = \begin{cases} 1 & s \geq \varphi \\ \dfrac{s}{\varphi} & -\kappa < s < \varphi \\ -1 & s \leq -\varphi \end{cases} \tag{19}$$

By this, there is a boundary layer φ around the sliding surface such that once the state trajectory reaches this layer, then it will be remaining there.

2.1.3 Fuzzy gain tuning

As mentioned before, by using a high gain in SMC, i.e. K, the sensitivity of the controller to the model uncertainties and external disturbances can be reduced. Moreover, a high gain in PID part of the control system (K_v) can reduce the reaching time to sliding surface and tracking error. However, increasing the gain causes the increment of the oscillations in the input torque around the sliding surface. Therefore, if this gain can be tuned based on the distance of the states to the sliding surface, a more acceptable performance can be achieved. In the other words, the value of gain should be selected high when the state trajectory is far from the sliding surface and when the distance is decreasing, its value should be decreased. This idea can be accomplished by using fuzzy logic in combination with SMC to tune the gain adaptively.

For this purpose, two-input one-output fuzzy system is designed whose inputs are s and $\dot{s}$ which are the distance of state trajectories to the sliding surface and its derivative, respectively. The membership functions of these two inputs are shown in Fig. 1. The output of the fuzzy system is denoted by K_{fuzz} and has been shown in Fig. 2. For applying these gains to the control input, the normalization factors N and N_v are used as the following relations:

$$K = N \cdot K_{fuzz} \tag{20}$$

$$K_v = N_v \cdot K_{fuzz} \tag{21}$$

These factors can be selected by trial and error such that the stability condition (17) is satisfied.

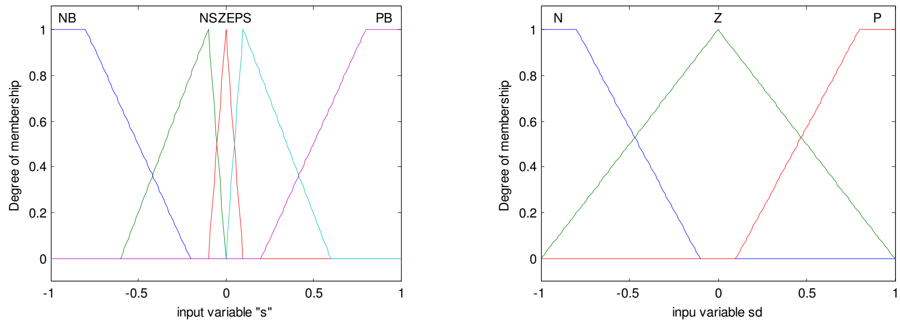

(a) (b)

Fig. 1. The membership functions, (a) input s, (b) input $\dot{s}$

The maximum values of K and K_v are limited according to the system actuators power, and the minimum value of K should not be less than the provided amount in relation (17). The fuzzy rule base has been given in table 1 in which the following abbreviations have been used: NB: Negative Big; NS: Negative Small; Z: Zero; PS: Positive Small; PB: Positive Big; M: Medium. For example, when s is negative small (*NS*) and $\dot{s}$ is positive (*P*), then K_{fuzz} is small (*S*).

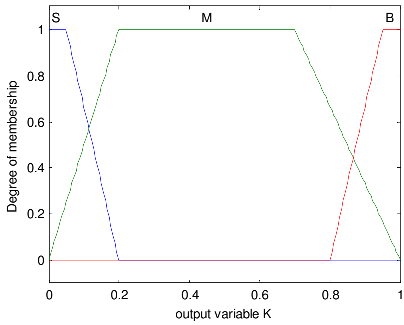

Fig. 2. The membership functions of the output K_{fuzz}

s \ $\dot{s}$	NB	NS	Z	PS	PB
N	B	B	M	S	B
Z	B	M	S	M	B
P	B	S	M	B	B

Table 1. The fuzzy rule base for tuning K_{fuzz}

Simulation example 2.1. In order to show the effectiveness of the proposed control law, it is applied to a two-link robot with the following parameters:

$$M(q)=\begin{bmatrix}\alpha+\beta+2\gamma\cos q_2 & \beta+\gamma\cos q_2\\ \beta+\gamma\cos q_2 & \beta\end{bmatrix} \tag{22}$$

$$C(q,\dot{q})=\begin{bmatrix}-\gamma\dot{q}_2\sin q_2 & -\gamma(\dot{q}_1+\dot{q}_2)\sin q_2\\ \gamma\dot{q}_1\sin q_2 & 0\end{bmatrix} \tag{23}$$

$$G(q)=\begin{bmatrix}\alpha\delta_1\cos q_1+\gamma\delta_1\cos(q_1+q_2)\\ \gamma\delta_1\cos(q_1+q_2)\end{bmatrix} \tag{24}$$

where $\alpha=(m_1+m_2)a_1^2$, $\beta=m_2a_2^2$, $\gamma=m_2a_1a_2$, $\delta=g/a_1$, and m_1 , m_2 , $a_1=.7$, $a_2=.5$ are the masses and lengths of the first and second links, respectively. The masses are assumed to be in the end of the arms and the gravity acceleration is considered as $g=9.8$. Moreover, the masses are considered with 10% uncertainty as follow:

$$\begin{aligned} m_1&=m_{1_0}+\Delta m_1,\ |\Delta m_1|\le .4\\ m_2&=m_{2_0}+\Delta m_2,\ |\Delta m_2|\le .2\end{aligned} \tag{25}$$

where $m_{1_0}=4$ and $m_{2_0}=2$, and $\hat{M}$, $\hat{C}$, and $\hat{G}$ are estimated. The desired state trajectory is:

$$q_d=\begin{bmatrix}1-\cos\pi t\\ 2\cos\pi t\end{bmatrix} \tag{26}$$

and the disturbance torque is considered as:

$$\tau_d = \begin{bmatrix} 0.5\sin 2\pi t \\ 0.5\sin 2\pi t \end{bmatrix} \tag{27}$$

which leads to $T_D = \begin{bmatrix} 0.5 \\ 0.5 \end{bmatrix}$.

The design parameters are determined as follow:

$$\lambda_1 = \begin{bmatrix} 15 & 0 \\ 0 & 15 \end{bmatrix},\ \lambda_2 = \begin{bmatrix} 40 & 0 \\ 0 & 40 \end{bmatrix} \tag{28}$$

Values of φ and η are selected as $\varphi = 0.167$ and $\eta = \begin{bmatrix} 0.1 & 0.1 \end{bmatrix}^T$. Moreover, the factors N and N_v are selected as:

$$N = \begin{bmatrix} 50 & 0 \\ 0 & 5 \end{bmatrix},\ N_v = \begin{bmatrix} 5 & 0 \\ 0 & 10 \end{bmatrix} \tag{29}$$

In order to show the improvement due to the proposed method, the simulation results of applying this method are compared with the related results of the conventional SMC. The tracking error and control law in the case of conventional SMC have been shown in Fig. 3 and Fig. 4, respectively. The corresponding graphs for the case of applying fuzzy SMC-PID are also provided in Fig. 5 and 6.

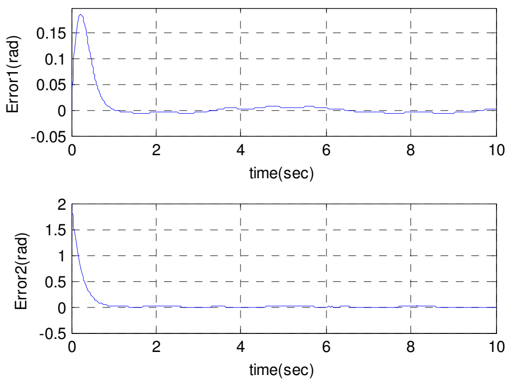

Fig. 3. The tracking errors in the case of using conventional SMC

As it can be seen from these figures, the proposed fuzzy SMC-PID has faster response and less tracking error in comparison with conventional SMC. In order to show more clearly the difference between the tracking errors in two cases, the enlarged graphs have been provided in Fig. 7 and 8.

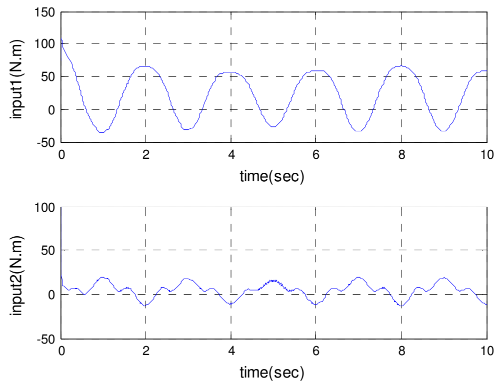

Fig. 4. The control inputs in the case of using conventional SMC

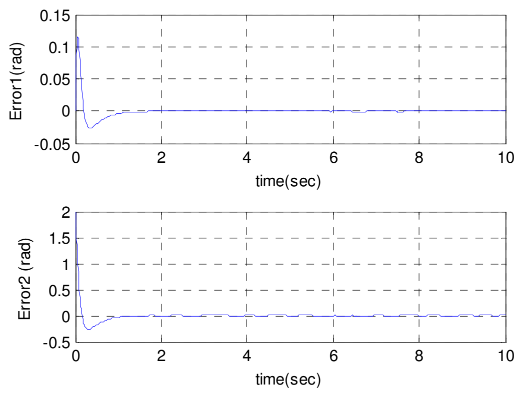

Fig. 5. The tracking errors in the case of using Fuzzy SMC-PID

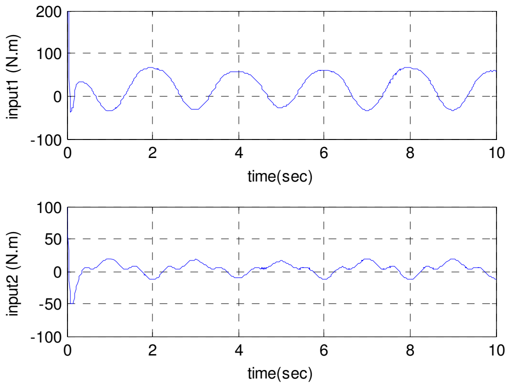

Fig. 6. The control inputs in the case of using Fuzzy SMC-PID

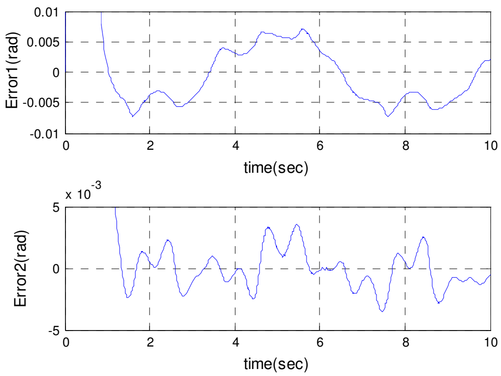

Fig. 7. The enlargement of the tracking errors in the case of using conventional SMC

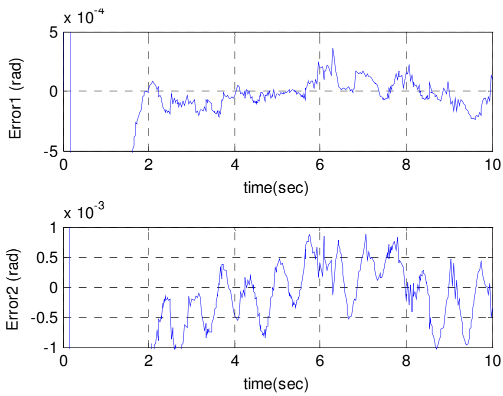

Fig. 8. The enlargement of the tracking errors in the case of using Fuzzy SMC-PID

2.2 Incorporating sliding mode and fuzzy control

In this section, a combined controller includes SMC term and fuzzy term is proposed for set-point tracking of robot manipulators. Some practical issues, such as existence of joint frictions, restriction on input torque magnitude due to saturation of actuators, and modeling uncertainties have been considered here. Design procedure contains two steps. First, SMC design is accomplished and system stability in this case is provided by Lyapunov direct method. When the tracking error would be less than predefined value then a sectorial fuzzy controller (SFC), (Calcev, 1998), is responsible for control action. Designing of this kind of fuzzy controller is exactly the same as in which has performed in (Santibanez et al., 2005).
This proposed controller has following advantages. 1) There are less tracking errors versus traditional SMC in condition that the control input is limited, 2) the chattering is avoided, 3) convergence of tracking error is more rapid than fuzzy controller designed in (Santibanez et al., 2005) and modeling uncertainty is considered here (Shafiei & Sepasi, 2010).

2.2.1 Mathematical model and problem formulation

This time the friction of joint is considered and is added to dynamical equation (1) as:

$$M(q)\ddot{q} + C(q,\dot{q})\dot{q} + G(q) + F(\dot{q},\tau) = \tau \tag{30}$$

where $F(\dot{q},\tau) \in R^n$ stands for the friction vector which is as follows (Cai & Song, 1994):

$$f_i(\dot{q},\tau_i) = b_i\dot{q}_i + f_{ci}\,\mathrm{sgn}(\dot{q}_i) + \left[1 - \left|\mathrm{sgn}(\dot{q}_i)\right|\right] sat(\tau_i; f_{si}) \tag{31}$$

where $f_i(\dot{q},\tau_i)$, $i = 1,2,\cdots,n$, denotes the i-th element of $F(\dot{q},\tau)$ vector. b_i, f_{ci} and f_{si} are the viscous, Coulomb and static friction, respectively. The sat(·; ·) indicates saturation function with following equation.

$$sat(x;r) = \begin{cases} r & if \quad x > r \\ x & if \quad -r \le x \le r \\ -r & if \quad x < -r \end{cases}$$

In the following, $M(q)$, $C(q,\dot{q})$ and $G(q)$ might be shown by M, C, and G, respectively in where it would be requisite.
Now, the boundedness properties are defined as below:

$$\sup_{q \in R^n} \left\{ \left| g_i(q) \right| \right\} \le \bar{g}_i, \quad i = 1,\cdots,n \tag{32}$$

where g_i stands for the i-th element of $G(q)$ and $\bar{g}_i$ is finite nonnegative constant. Assume that the maximum torque that joint actuator can supply is $\tau^{\max}$. Therefore:

$$\left|\tau_i\right| \le \tau_i^{\max}, \quad i = 1,\cdots,n \tag{33}$$

and each actuator satisfies the following condition:

$$\tau_i^{\max} > \bar{g}_i + f_{si} \tag{34}$$

In robot modeling, one can well determine the terms $M(q)$ and $G(q)$ but it is difficult in most cases obtaining the parameters of $C(q,\dot{q})$ and $F(\dot{q},\tau)$ exactly. So, in present section, the matrix C is considered as follows:

$$C = \hat{C} + \Delta C \tag{35}$$

where $\hat{C}$ denotes estimation of C, and ΔC is bounded estimation error which has the following relation:

$$\left|\Delta C_{i,j}\right| \le 0.1\left|C_{i,j}\right| \tag{36}$$

where $C_{i,j}$ stands for elements of the matrix C. Also the vector F is supposed as an external disturbance with the following unknown upper bound:

$$\|F\| \le F_{up} \tag{37}$$

where the operator $\|\cdot\|$ denotes Euclidean norm.

If one considers the desired point which joint position must be held on it as q_d, then the position error could be defined as:

$$\tilde{q} = q_d - q \tag{38}$$

Here, the set-point tracking problem refers to define the control law such that error e would be driven toward the inside of an arbitrary small region around zero with maintaining the torques within the constraints (33). In succeeding subsections, this aim will be attained.

2.2.2 Sliding mode controller design

The following sliding surface is considered for designing SMC controller.

$$s = \dot{e} + \lambda e \tag{39}$$

where $e = -\tilde{q} = q - q_d$ is error vector and λ is supposed symmetric positive definite matrix such that s=0 would become a stable surface. The reference velocity vector "$\dot{q}_r$" is defined as in (Slotin & Li, 1991):

$$\dot{q}_r = \dot{q}_d - \lambda e \tag{40}$$

Thus, one can interpret sliding surface as:

$$s = \dot{q} - \dot{q}_r \tag{41}$$

Here, the SMC controller design is expressed by lemma 2.2.

Lemma 2.2. Consider the system with dynamic equation (30) and sliding surface and reference velocity defined by (39) and (40), respectively. If one chooses the control law below,

$$\tau = \hat{\tau} - K\,\mathrm{sgn}(s) \tag{42}$$

such that

$$\hat{\tau} = M\ddot{q}_r + \hat{C}\dot{q}_r + G \tag{43}$$

and

$$K_i \geq \left\| \Delta C\dot{q}_r \right\| + \Gamma_i \tag{44}$$

then the sliding condition (10) is satisfied. In the last inequality, K_i denotes the element of sliding gain vector K and Γ is design parameter vector which must be selected such that $\Gamma_i \geq F_{up} + \eta_i$.

Proof: Consider the following Lyapunov function candidate:

$$V = \frac{1}{2}s^T M s \tag{45}$$

Since M is positive definite, for $s \neq 0$ we have $V > 0$ and by taking time derivative of the relation (45) and regarding the symmetric property of M, it can be written:

$$\dot{V} = s^T M\dot{s} + \frac{1}{2}s^T \dot{M}s \tag{46}$$

from (40), gives:

$$\dot{V} = s^T (M\ddot{q} - M\ddot{q}_r) + \frac{1}{2}s^T \dot{M}s \tag{47}$$

By substituting (30) in (47) and considering asymmetry property $s^T(\dot{M} - 2C)s = 0$, we have:

$$\dot{V} = s^T (\tau - C\dot{q}_r - G - F - M\ddot{q}_r) \tag{48}$$

Now, applying (42) and (43) yields:

$$\dot{V} = s^T (\Delta C\dot{q}_r + F) - \sum_{i=1}^{n} K_i |s_i| \tag{49}$$

Finally, from relation (44) it can be concluded that:

$$\dot{V} \leq -\sum_{i=1}^{n} \eta_i |s_i| \tag{50}$$

This indicates that V is a Lyapunov function and the sliding condition (10) has been satisfied.

Note that, in general, the sign function is replaced by saturation function as $\mathrm{sat}(s/\varphi)$, where φ denotes boundary layer thickness.

2.2.3 Fuzzy controller design

In this section, the SFC class of fuzzy controller studied in (Santibanez et al., 2005) is considered which has two-input one-output rules used in the formulation of the knowledge base. These IF-THEN rules have following form:

$$\text{IF}\, x_1 \,\text{is}\, A_1^{l_1} \,\text{and}\, x_2 \,\text{is}\, A_2^{l_2} \,\text{THEN}\, y \,\text{is}\, B^{l_1 l_2} \tag{51}$$

where $x = [x_1 \quad x_2]^T \in U = U_1 \times U_2 \subset \Re^2$ and $y \in V \subset \Re$. For each input fuzzy set $A_j^{l_j}$ in $x_j \subset U_j$ and output fuzzy set $B^{l_1 l_2}$ in $y \subset V$, exist an input membership function $\mu_{A_j^{l_j}}(x_j)$ and output membership function $\mu_{B^{l_1 l_2}}(y)$ shown in Fig. 10 and Fig. 11, respectively.

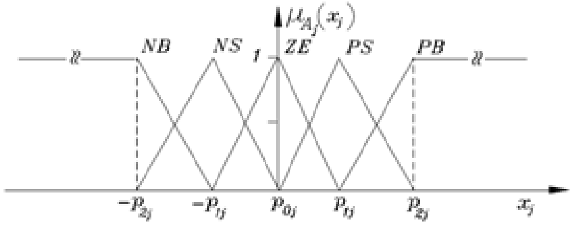

Fig. 9. Input membership functions

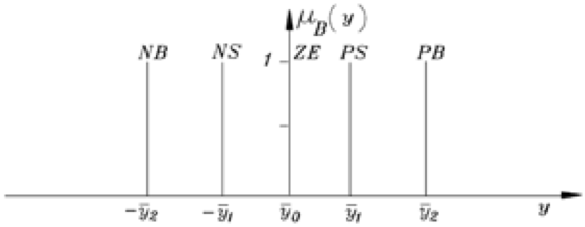

Fig. 10. Output membership functions

The fuzzy system considered here has following specifications: Singleton fuzzifier, triangular membership functions for each inputs, singleton membership functions for the output, rule base defined by (51), (see Table. 2), product inference and center average defuzzifier.

x_2 \ x_1	NB	NS	ZE	PS	PB
NB	NB	NB	NS	ZE	ZE
NS	NB	NB	NS	ZE	ZE
ZE	NS	NS	ZE	PS	PS
PS	ZE	ZE	PS	PB	PB
PB	ZE	ZE	PS	PB	PB

Table 2. The fuzzy rule base for obtaining output y

Thus, one can compute the output y in terms of inputs as follows (Wang, 1997):

$$y(x) = \varphi(x_1, x_2) = \frac{\sum_{l_1}\sum_{l_2} \bar{y}^{l_1 l_2}\left(\bigcap_{j=1}^{2} \mu_{A_j^{l_j}}(x_j)\right)}{\sum_{l_1}\sum_{l_2}\left(\bigcap_{j=1}^{2} \mu_{A_j^{l_j}}(x_j)\right)} \tag{52}$$

Special properties of this input-output mapping $y(x)$ for x_1, x_2 are given in (Santibanez et al., 2005).

Lemma 2.3. For the system with dynamical equation (30), if one chooses the following control law,

$$\tau = \varphi(\tilde{q},\dot{\tilde{q}}) + G(q) \tag{53}$$

where $\tilde{q}$ is defined as (38) and $\dot{\tilde{q}} = \dot{q}_d - \dot{q}$ is velocity error vector, then the closed-loop system shown in Fig. 11 becomes stable.

Proof: the stability analysis is based on the study performed in (Calcev 1998) and is fully discussed in (Santibanez et al., 2005), so it is omitted here. Note that for constant set-point we have $\dot{q}_d = 0$, hence $\dot{\tilde{q}} = -\dot{q}$.

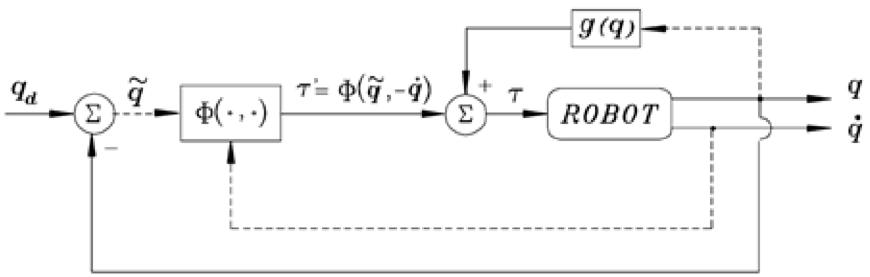

Fig. 11. Closed-loop system in the case of fuzzy controller (Santibanez et al., 2005)

2.2.4 Incorporating SMC and SFC

Each of the two controllers explained in last two subsections drives the robot joint angles to desired set-point in finite time and according to the Lemma 2.2 and 2.3 the closed-loop system is stable in both cases. In this section, for utilizing advantages of both sliding mode control and sectorial fuzzy control, and also minimizing the drawbacks of both of them, the following control law is proposed:

$$\tau = \begin{cases} \hat{\tau} - K\operatorname{sgn}(s) & \text{when} \left|\mathrm{q_e}\right| \geq \alpha \\ y(q_e,\dot{q}_e) + G(q) & \text{when} \left|\mathrm{q_e}\right| < \alpha \end{cases} \tag{54}$$

where α is strictly positive small parameter which can be determined adaptively or set to a constant value. So, while the magnitude of error is greater than or equal to α, SMC drives the system states, errors in our case, toward sliding surface and as soon as the magnitude of error becomes less than α, then the SFC which is designed independent of initial conditions, controls the system. Since the SMC shows faster transient response, the response of the system controlled by (54) is faster than the case of SFC. Additionally, in spite of the torque boundedness, since the SFC controls the system in the steady state, the proposed controller (54) has less set-point tracking error. Also, since near the sliding surface the proposed controller switch from SMC to SFC, therefore, the chattering is avoided here.

Simulation example 2.2. In order to show the effectiveness of the proposed control law, it is applied to a two-link direct drive robot arm with the following parameters (Santibanez et al., 2005):

$$\begin{aligned}
M(q) &= \begin{bmatrix} 2.351 + 0.168\cos(q_2) & 0.102 + 0.084\cos(q_2) \\ 0.102 + 0.084\cos(q_2) & 0.102 \end{bmatrix} \\
\hat{C}(q,\dot{q}) &= \begin{bmatrix} -0.084\sin(q_2)\dot{q}_2 & -0.084\sin(q_2)(\dot{q}_1 + \dot{q}_2) \\ 0.084\sin(q_2)\dot{q}_1 & 0 \end{bmatrix} \\
G(q) &= 9.81\begin{bmatrix} 3.921\sin(q_1) + 0.186\sin(q_1 + q_2) \\ 0.186\sin(q_1 + q_2) \end{bmatrix} \\
F(\dot{q}) &= \begin{bmatrix} 2.288\dot{q}_1 + 8.049\,\mathrm{sgn}(\dot{q}_1) + \left[1 - \left|\mathrm{sgn}(\dot{q}_1)\right|\right]\mathrm{sat}(\tau_1; 9.7) \\ 0.186\dot{q}_2 + 1.734\,\mathrm{sgn}(\dot{q}_2) + \left[1 - \left|\mathrm{sgn}(\dot{q}_2)\right|\right]\mathrm{sat}(\tau_2; 1.87) \end{bmatrix} \\
C &= \hat{C} + \Delta C
\end{aligned} \tag{55}$$

According to the actuators manufacturer, the direct drive motors are able to supply torques within the following bounds:

$$\begin{aligned} |\tau_1| &\le \tau_1^{\max} = 150[\mathrm{Nm}] \\ |\tau_2| &\le \tau_2^{\max} = 15[\mathrm{Nm}] \end{aligned} \tag{56}$$

The desired set-point is,

$$q_d = \begin{bmatrix} \pi & -\pi \end{bmatrix}^T \tag{57}$$

which is applied as a step function at time zero. The SMC design parameters are as below:

$$\lambda = \begin{bmatrix} 10 & 0 \\ 0 & 10 \end{bmatrix},\ \Gamma = \begin{bmatrix} 140 \\ 8 \end{bmatrix} \text{ and } \phi = 5 \tag{58}$$

For SFC case, according to Fig. 9 and Fig. 11, $p_{x_j} = \{-p_{2j}, -p_{1j}, p_{0j}, p_{1j}, p_{2j}\}$ is fuzzy partition of the input universe of discourse and $p_y = \{-\overline{y}_2, -\overline{y}_1, \overline{y}_0, \overline{y}_1, \overline{y}_2\}$ is for output universe of discourse. Now, SFC design parameters are given by following equations (Santibanez et al., 2005):

$$\begin{aligned}
p_{\tilde{q}_1} &= \{-180, -4, 0, 4, 180\} \\
p_{\tilde{q}_2} &= \{-180, -2, 0, 2, 180\} \\
p_{\dot{\tilde{q}}_1} &= \{-360, -270, 0, 270, 360\} \\
p_{\dot{\tilde{q}}_2} &= \{-360, -270, 0, 270, 360\} \\
p_{y_1} &= \{-109, -90, 0, 90, 109\} \\
p_{y_2} &= \{-13, -9, 0, 9, 13\}
\end{aligned} \tag{59}$$

For our proposed controller (54), the constant $\alpha = 0.3$ is supposed. Additionally, to show the improvement achieved from applying the proposed method of this section (incorporating

SMC and SFC), the simulation results of applying this method are compared with the related results of the SMC case and SFC case, separately. The error vector and control law in the case of conventional SMC have been shown in Fig. 12 and Fig. 13, respectively.

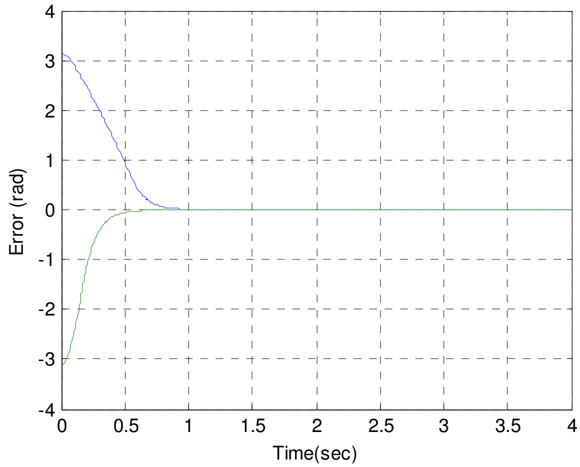

Fig. 12. Error vector in the case of SMC

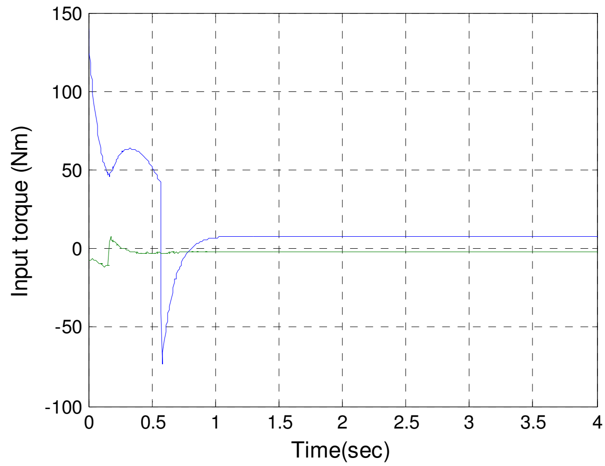

Fig. 13. The control torques in the case of SMC

The tracking error in this case is about 0.1(rad) and when one choose the thinner boundary layer to decrease this error, chattering will be occurred. The corresponding graphs for the case of applying SFC are also provided in Fig. 14, and Fig. 15.

In the case of control law proposed in the present section, Fig. 16 and Fig. 17 illustrate the error vector and control law, respectively. The tracking error is about 0.002 in this state of affairs.